



Bidirectional real-time hybrid test on a steel column virtually connected to a reinforced concrete substructure

Bastien Bodnar, Magdalini Titirla, Fabrice Gatuingt, Frédéric Ragueneau,
Jean-François Deü

► To cite this version:

Bastien Bodnar, Magdalini Titirla, Fabrice Gatuingt, Frédéric Ragueneau, Jean-François Deü. Bidirectional real-time hybrid test on a steel column virtually connected to a reinforced concrete substructure. EURODEX 2023 - XII International Conference on Structural Dynamics, Jul 2023, Delft, Netherlands. 10.1088/1742-6596/2647/14/142007 . hal-04303424v2

HAL Id: hal-04303424

<https://hal.science/hal-04303424v2>

Submitted on 4 Jul 2024

HAL is a multi-disciplinary open access archive for the deposit and dissemination of scientific research documents, whether they are published or not. The documents may come from teaching and research institutions in France or abroad, or from public or private research centers.

L'archive ouverte pluridisciplinaire **HAL**, est destinée au dépôt et à la diffusion de documents scientifiques de niveau recherche, publiés ou non, émanant des établissements d'enseignement et de recherche français ou étrangers, des laboratoires publics ou privés.

BIDIRECTIONAL REAL-TIME HYBRID TEST ON A STEEL COLUMN VIRTUALLY CONNECTED TO A REINFORCED CONCRETE SUBSTRUCTURE

B. Bodnar^{1,2}, M. Titirla¹, F. Gatuingt², F. Ragueneau^{2,3}, W. Larbi¹ and J.-F. Deü¹

¹ Conservatoire National des Arts et Métiers, Laboratoire de Mécanique des Structures et des Systèmes Couplés, 292 rue Saint-Martin, 75141 Paris cedex 03, France

² Université Paris-Saclay, Centrale Supélec, ENS Paris-Saclay, CNRS, Laboratoire de Mécanique Paris-Saclay, 91190, Gif-sur-Yvette, France

³ EPF École d'Ingénieurs, 55 av. Président Wilson, F-94230, Cachan, France

bastien.bodnar@lecnam.net; magdalini.titirla@lecnam.net;
fabrice.gatuingt@ens-paris-saclay.fr; frederic.ragueneau@ens-paris-saclay.fr;
walid.larbi@lecnam.net; jean-francois.deu@cnam.fr

Abstract. This paper uses a hyper-reduced order model (HROM) to perform bidirectional Hardware-in-the-Loop (HiL) real-time hybrid tests on a steel column virtually connected to a two-story reinforced concrete (RC) substructure under earthquake conditions. Two hydraulic dynamic actuators apply the horizontal displacements at the top of the specimen. Nonlinear multi-fiber beam elements are used to model the numerical substructure. The computational cost of the finite element (FEM) analysis is reduced using a Proper Orthogonal Decomposition (POD) Unassembled Discrete Empirical Interpolation Method (UDEIM) with a non-iterative α -Operator Splitting (α -OS) time integration scheme. Data acquisition is carried out using a Linux[®] real-time (RT) target, while the dynamic analysis is performed on a Windows[®] host computer running custom procedures implemented in MATLAB[®] software. A LABVIEW[®] interface connects both systems via a lossless stream network. Results on the present case study show that: (1) using a HROM can accelerate costly nonlinear dynamic analyses so that they can be run above the sampling period of the ground motion during hybrid tests, and (2) using lossless stream networks calling a MATLAB[®] kernel efficiently combines the high data acquisition speed of RT targets (i.e., 10 μ s per sample) with the computing power of host computers since the data exchange is quasi-instantaneous.

1. Introduction

Tests on sensitive structural elements (e.g., columns, beams, or frames) are sometimes necessary to study the behavior of civil engineering structures (e.g., dynamic response, damage, or failure mechanisms) under earthquake conditions. Quasi-static “push-over” or dynamic tests are carried out for this purpose. However, these approaches are limited since it is not possible to experimentally consider the inertial forces as well as cyclic loadings during “push-over” tests, while the similitude theory leads to the addition of masses on the small-scale specimens during dynamic experiments on shaking tables or in centrifuge facilities. As a result, unrealistic collapse mechanisms may appear.

To overcome these limitations, “hybrid tests” have been developed over the last decades. They allow for the assessment of the dynamic response of specimens at full scale considering numerically the

environment in which they are installed. The commands of the actuators loading the specimen are computed through a dynamic analysis carried out simultaneously on a numerical model including all the untested components.

A common approach, called Pseudo-Dynamic (PsD), consist of applying the displacements in deferred time [1]. Such experiments are easier to perform than Real-Time (RT) hybrid tests since the real time can only be reached provided that the delay of the overall process (including the FEM analysis, the movement of the actuators, the measurements, and the data exchange) is lower than the sampling period of the ground motion (i.e., approximately equal to 10 ms). This can be difficult to achieve since nonlinear material laws are required to accurately consider the decrease of stiffness due to damage during earthquakes. To avoid iterating and prevent the risk of overshoot (i.e., sudden collapse of the specimen), an Operator Splitting (OS) method was developed [2]. The restoring force vector is split into a nonlinear term based on an explicit prediction of the displacements and a linear term depending on the elastic stiffness matrix. This integration scheme, called α -OS, was successfully applied to perform PsD hybrid tests using in-plane numerical substructures made of linear elements [3], elastic-plastic hinges [4], or multifibre beam elements ([5], [6]), while only linear elements or nonlinear macro elements were used in real time [7]. To the best of our knowledge, the use of semi-global approaches (e.g., multifibre beam elements, or multilayer shell elements) to carry out RT hybrid tests using out-of-plane models has not been investigated yet due to their computational cost, even if recent advances in Reduced Order Modelling (ROM) could advantageously be used to decrease the delay of Hardware-in-the-Loop (HiL) procedures involving high dimensional nonlinear systems. *A posteriori* methods are useful here since the properties of the external loading, the tested specimen, and the numerical substructure are all known so that accurate snapshots can be pre-computed. A modal basis can be built using a Proper Orthogonal Decomposition (POD) method [8]. In addition, the computational cost due to the assessment of the nonlinear terms of the matrix system can be reduced using hyper reduction procedures such as the Unassembled Discrete Empirical Interpolation Method (UDEIM) [9]. The UDEIM consists of approximating the nonlinear terms based on samples assessed on a set of elements belonging to a Reduced Integration Domain (RID). Such a method drastically reduces the computational cost of FEM analyses since only a small number of elements needs to be updated during the online phase, making Hyper Reduced Order Models (HROMs) useful to decrease the delay of hybrid tests procedures.

Efficient measurement devices guaranteeing a quasi-instantaneous data acquisition also need to be used to successfully perform RT hybrid tests. Embedded Linux[®] RT targets meet this requirement since they are able to measure and read data on demand with a delay approximately equal 10 μ s. A host computer and a lossless exchange network that ensure high speed data transfers with the RT target (e.g., stream network) are also required to simultaneously run the FEM analysis in real time.

This paper presents the results of a bi-directional HiL real-time hybrid test on a steel column virtually connected at its top to a two-story RC structure under earthquake conditions. The study emphasizes on efficiently integrating the finite element solver in the testing procedure, reducing the computational cost of the simulated substructure, and ensuring quasi-instantaneous data exchange between the components of the experimental setup. To the best of our knowledge, the use of hyper-reduced order modeling methods to perform real-time HiL hybrid tests has not been investigated yet. In Section 2, the non-iterative α -OS time scheme and the substructuring method are detailed. The Section 3 summarizes the POD-UDEIM hyper reduction procedure. The case study, the experimental set up, and its components (e.g., host computer, Linux[®] RT target, and actuators) are described in Section 4. The Section 5 presents the HROM (i.e., number of modes, time-savings), a benchmark comparison of the methods available in LabVIEW[®] for running FEM analyses, and experimental results (e.g., delays, or comparison between the commands and the displacements).

2. Time integration scheme and substructuring method

The α -OS time integration scheme is based on the classical Hilber-Hugues-Taylor (HHT) method [10] and consists of splitting the restoring force vector into a nonlinear part $\tilde{\mathbf{r}}^{\text{NL}}(\tilde{\mathbf{u}})$ approximated using an explicit prediction of the displacements, and a linear part depending on the elastic stiffness matrix (1):

$$\mathbf{r}(\mathbf{u}) \cong \mathbf{K}_E \mathbf{u} + \tilde{\mathbf{r}}^{\text{NL}}(\tilde{\mathbf{u}}) \quad \text{with} \quad \tilde{\mathbf{r}}^{\text{NL}}(\tilde{\mathbf{u}}) = \tilde{\mathbf{r}}(\tilde{\mathbf{u}}) - \mathbf{K}_E \tilde{\mathbf{u}} \quad (1)$$

where \mathbf{K}_E is the elastic stiffness matrix, \mathbf{u} is the displacement vector, $\tilde{\mathbf{u}}$ is the explicit prediction of the displacement vector, and $\tilde{\mathbf{r}}(\tilde{\mathbf{u}})$ is the prediction of the restoring force vector. The system of linear equations to be solved to compute $\ddot{\mathbf{u}}_{n+1}$ at time step $n + 1$ is thus given in (2) by introducing (1) into the equation of motion:

$$\hat{\mathbf{M}} \ddot{\mathbf{u}}_{n+1} = \hat{\mathbf{F}}_{n+1+\alpha} \quad (2)$$

where $\hat{\mathbf{M}}$ is the pseudo mass matrix, and $\hat{\mathbf{F}}_{n+1+\alpha}$ is the pseudo force vector [11]. One can note that the method depends on an α parameter set between -1/3 and 0, and usually close to -0.05 [10]. During hybrid tests, the high frequency content due to the measurement noise is thus dampened. As demonstrated in practical cases, the residual error due to the approximation in (1) is almost negligible in the case of dynamic FEM analyses on RC structures subjected to infinitesimal strains [12].

The numerical substructure and the tested specimen are then split to introduce the restoring forces applied by the actuators as external loads on the common DOFs, as shown in the example in Figure 1.

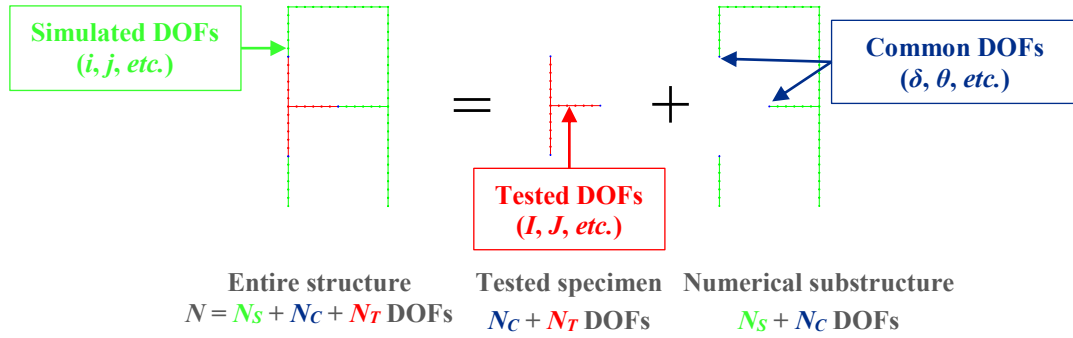


Figure 1: Substructuring of an in-plane two-story frame.

Among the N DOFs, N_S DOFs only belong to the modelled substructure (subscript I and j), N_C belong to both the modelled substructure and the tested specimen (subscript δ and θ), and N_T only belong to the tested specimen (subscript I and J). By distinguishing in (2) the systems of equations coming from the numerical substructure (subscripted S), and the tested specimen (subscripted T), it is possible to reorganize the matrix $\hat{\mathbf{M}}$ and the related terms as described in (3):

$$\begin{bmatrix} {}^S\hat{\mathbf{M}}_{ij} & {}^S\hat{\mathbf{M}}_{i\theta} & \mathbf{0} \\ {}^S\hat{\mathbf{M}}_{\delta j} & {}^S\hat{\mathbf{M}}_{\delta\theta} + {}^T\hat{\mathbf{M}}_{\delta\theta} & {}^T\hat{\mathbf{M}}_{\delta J} \\ \mathbf{0} & {}^T\hat{\mathbf{M}}_{I\theta} & {}^T\hat{\mathbf{M}}_{IJ} \end{bmatrix} \begin{bmatrix} \ddot{\mathbf{u}}_{j,n+1} \\ \ddot{\mathbf{u}}_{\theta,n+1} \\ \ddot{\mathbf{u}}_{J,n+1} \end{bmatrix} = \begin{bmatrix} {}^S\hat{\mathbf{F}}_{i,n+1+\alpha} \\ {}^S\hat{\mathbf{F}}_{\delta,n+1+\alpha} + {}^T\hat{\mathbf{F}}_{\delta,n+1+\alpha} \\ {}^T\hat{\mathbf{F}}_{I,n+1+\alpha} \end{bmatrix} \quad (3)$$

where $\ddot{\mathbf{u}}_{j,n+1}$, $\ddot{\mathbf{u}}_{\theta,n+1}$ and $\ddot{\mathbf{u}}_{J,n+1}$ are the acceleration vectors related to the simulated, common, and tested DOFs, respectively. The measured restoring force vector ${}^T\tilde{\mathbf{r}}_{\delta,n+1}$ is introduced in the pseudo force vector ${}^T\hat{\mathbf{F}}_{\delta,n+1+\alpha}$, whereas the restoring force vectors computed on the numerical substructure ${}^S\tilde{\mathbf{r}}_{i,n+1}$ and ${}^S\tilde{\mathbf{r}}_{\delta,n+1}$ are introduced in ${}^S\hat{\mathbf{F}}_{i,n+1+\alpha}$ and ${}^S\hat{\mathbf{F}}_{\delta,n+1+\alpha}$, respectively [11].

At the time step $n + 1$, the matrix system in (3) is first reduced by condensing the components of $\ddot{\mathbf{u}}_{j,n+1}$ so that the entries of the acceleration vector can be computed on the common DOFs. Once $\ddot{\mathbf{u}}_{\theta,n+1}$ is known, the entries related to the simulated DOFs (stored in $\ddot{\mathbf{u}}_{j,n+1}$) are then assessed by solving the equations indexed i in (3).

3. Reduced order modelling using a POD-UDEIM approach

This paper proposes to reduce the computational cost of the simulated substructure using a POD method combined with a UDEIM approach. Nonlinear FEM analyses are first performed on a Full Order Model (FOM) including both the numerical and the tested components. Displacement snapshots are then used as training data to compute nonlinear POD modes by carrying out a Singular Value Decomposition (SVD) on the simulated DOFs. The n first POD modes are then selected to build a reduced modal basis. This a posteriori approach reduces the number of DOFs as well as the computational cost of the matrix operations. The displacement vector related to the simulated substructure ${}^S\mathbf{u} \in \mathbb{R}^{N_S+N_C}$ can thus be expressed according to a new POD basis $\Phi \in \mathbb{R}^{N_S \times n}$, as described in (4):

$${}^S\mathbf{u} = \begin{pmatrix} \mathbf{u}_j \\ \mathbf{u}_\theta \end{pmatrix} \approx \Gamma {}^S\mathbf{q} \quad \text{with} \quad \Gamma = \begin{bmatrix} \Phi & \mathbf{0} \\ \mathbf{0} & I_d \end{bmatrix}, \quad {}^S\mathbf{q} = \begin{pmatrix} \mathbf{q}_j \\ \mathbf{u}_\theta \end{pmatrix}, \quad \text{and} \quad \Phi = [\boldsymbol{\varphi}_1 \quad \cdots \quad \boldsymbol{\varphi}_n] \quad (4)$$

where $\mathbf{q}_j \in \mathbb{R}^n$ is the displacement vector related to the N_S simulated DOFs in the reduced basis Φ , $\boldsymbol{\varphi}_{i=1,\dots,n} \in \mathbb{R}^{N_S}$ is the i^{th} POD mode computed using a SVD procedure, and $I_d \in \mathbb{R}^{N_C \times N_C}$ is an identity matrix. In addition, a UDEIM interpolation operator is here added to the solving process. To do so, a second SVD is performed on the force snapshots related to the nonlinear parts of the unassembled restoring force vector (i.e., computed element per element) (5):

$${}^S\tilde{\mathbf{r}}^{\text{NL,u}}({}^S\mathbf{u}) = {}^S\tilde{\mathbf{r}}^{\text{u}}({}^S\mathbf{u}) - \mathbf{K}_E^{\text{u}} \mathbf{B} \begin{pmatrix} \tilde{\mathbf{u}}_j \\ \tilde{\mathbf{u}}_\theta \end{pmatrix} \quad (5)$$

where N_e is the number of simulated finite elements, N_f is the number of force entries per element, $\mathbf{K}_E^{\text{u}} \in \mathbb{R}^{N_e \cdot N_f \times N_e \cdot N_f}$ is the unassembled elastic stiffness matrix of the simulated substructure, $\mathbf{B} = [\mathbf{L}_1^T \quad \cdots \quad \mathbf{L}_{N_e}^T]^T \in \mathbb{R}^{N_e \cdot N_f \times (N_S+N_C)}$ is a Boolean assembly matrix, $\mathbf{L}_{e=1,\dots,N_e} \in \mathbb{R}^{N_f \times (N_S+N_C)}$ is a collocation matrix used to select the displacements of the nodes connected to the e^{th} finite element, and $\tilde{\mathbf{u}}_j$ and $\tilde{\mathbf{u}}_\theta$ are the explicit predictions of the displacement on the simulated and common DOFs, respectively. The m first force modes are then selected to build a second truncated modal basis $\Psi = [\boldsymbol{\psi}_1 \quad \cdots \quad \boldsymbol{\psi}_m] \in \mathbb{R}^{N_e \cdot N_f \times m}$. A DEIM algorithm is next to find for each UDEIM mode $\boldsymbol{\psi}_i \in \mathbb{R}^{N_e \cdot N_f}$ the best collocation entries [15]. The material laws are updated on the elements belonging to the RID (i.e., where the nonlinear part of the unassembled restoring force vector needs to be computed). The k collocation entries belonging to the RID are then used as samples to build an explicit prediction of the reduced restoring force vector ${}^S\tilde{\mathbf{r}} \in \mathbb{R}^{n+N_C}$, as described in (6):

$${}^S\tilde{\mathbf{r}}(\Gamma {}^S\tilde{\mathbf{q}}) = \Gamma^T \mathbf{B}^T \left((I_d - \mathbf{A} \mathbf{P}^T) \mathbf{K}_E^{\text{u}} \mathbf{B} \Gamma {}^S\tilde{\mathbf{q}} + \mathbf{A} {}^S\tilde{\mathbf{r}}_{\text{RID}}(\Gamma {}^S\tilde{\mathbf{q}}) \right) \quad (6)$$

with $\mathbf{A} = \Psi(\mathbf{P}^T \Psi)^+$

where $\mathbf{P} \in \mathbb{R}^{N_e \cdot N_f \times k}$ is a Boolean partition matrix that refers the k collocation entries, $\Gamma \in \mathbb{R}^{(n+N_C) \times (N_S+N_C)}$ is the reduced basis related to the numerical substructure, ${}^S\tilde{\mathbf{q}} \in \mathbb{R}^{n+N_C}$ is the approximation of the displacement vector in basis Γ , and $\mathbf{A} \in \mathbb{R}^{N_e \cdot N_f \times k}$ is the UDEIM interpolation operator. Thus, the CPU time related to the simulated substructure can be considerably reduced since only the internal variables of the elements belonging to the RID need to be updated.

4. Case study and experimental setup

4.1. Case study

The case study consisted of a tested steel column virtually connected to the southeast corner of a two-story RC building (see Figure 2 (a)) loaded by the ground motion in Figure 2 (b). The specimen was embedded to a reaction wall *via* an end plate, and was loaded at its top by two dynamic actuators modeling a bidirectional pin connection along the x and y -axes. The vertical displacement and force entries (i.e., along the z -axis) were computed numerically to simplify the experimental setup.

A 3 m long HEA 200 steel column was taken as a tested specimen. Half of its mass $M = 63.5$ kg with elastic stiffnesses $K_{xx} = 545 \times 10^3$ N/m, $K_{yy} = 169 \times 10^3$ N/m, and $K_{zz} = 377 \times 10^6$ N/m modeled its action on the common DOFs (subscript δ and θ) using the pseudo mass matrix ${}^T\hat{\mathbf{M}}_{\delta\theta}$ (3). K_{xx} and K_{yy} were directly measured on the experimental setup, and no tested DOF (subscript I and J) was taken into account since the steel column was embedded to the ground level. Adding half the mass of the specimen to ${}^T\hat{\mathbf{M}}_{\delta\theta}$ made it possible to compensate for the inertia of the steel column since its effect cannot be directly measured on the experimental set up.

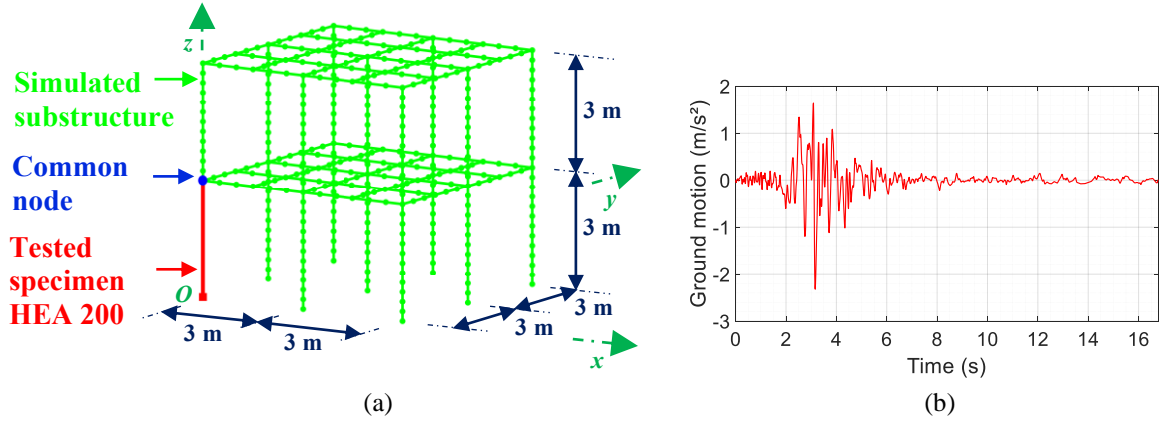


Figure 2: Mesh of the building (a), and ground acceleration versus time (b).

The numerical substructure was modeled by 405 nodes linked by 444 multifibre beam elements [13]. All the columns were embedded to the floor level, and 2382 free DOFs modeled the building (see Figure 2 (a)). A mass per unit area of 500 kg/m² was applied to both floors. Masses were first allocated proportionally to the nodes connecting the transversal and the longitudinal beams to be then distributed linearly to the intermediate nodes. The columns had a 15 × 15 cm square cross-section, and the beams had a 15 × 25 cm rectangular one (see Figure 3 (a)). The cross-sections of the beams and the columns were divided into 3 × 5 and 3 × 3 surface elements, respectively (see Figure 3 (b)).

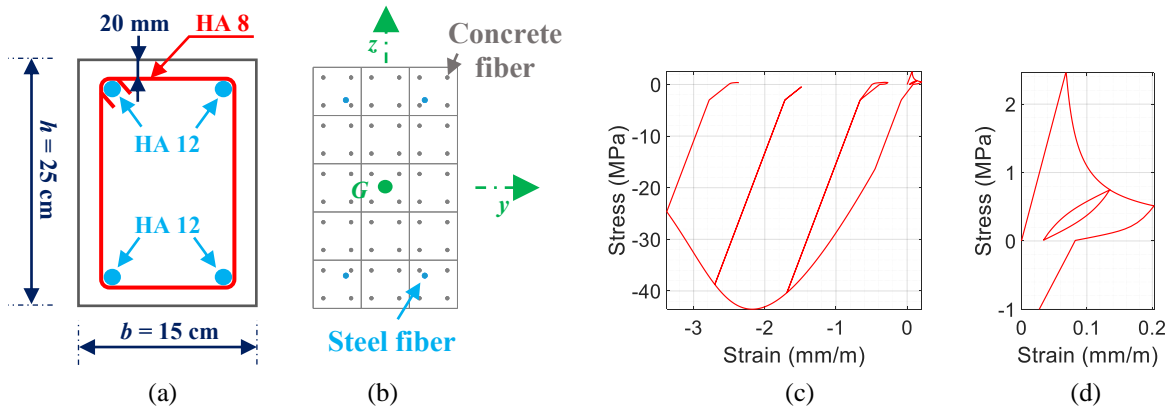


Figure 3: Steel reinforcements (a) and mesh (b) of the beam cross-sections, and uniaxial damage law for concrete with opening/closing of cracks (c) and frictional sliding (d).

Knowing that the length/height ratio of the structural components (e.g., beams, or columns) is usually higher than 10 in civil engineering structures, the damage was assumed to be mainly due to bending. A “unilateral” damage law with frictional sliding developed to model quasi-brittle materials under dynamic or cyclic loadings [14] was used for concrete fibers (see Figure 3 (c) & (d)), while a bilinear elastic-plastic law modeled the steel rebars, with an elastic modulus of 210 GPa, a yielding stress of

500 MPa, and a kinematic hardening of 1 GPa. A Rayleigh viscous damping ratio modeled the structural damping due to the viscosity of air and materials, or discontinuities at junctions. It was set at $\xi = 2\%$ at $f_1 = 1.47$ Hz (eigenfrequency #1) and $f_6 = 5.50$ Hz (eigenfrequency #6) so that its value reached a minimum around the main eigenmodes. Factors equal to 1.10 in the x-direction, 0.50 in the y-direction, and 0.30 in the z-direction weighed the ground motion in Figure 2 (b), while the dead and live loads were statically applied before entering the time step loop.

4.2. Experimental setup

The experiment was performed on the RESIST testing platform of the LMPS laboratory (see Figure 4 (a)). The HEA 200 steel column was set up horizontally, and embedded to a reaction wall *via* an end plate. Two horizontal and vertical dynamic actuators equipped with accumulators and pin connected to a frame structure loaded the steel column along the x and y -axes, respectively. Both had a maximum capacity of 250 kN, a stroke of ± 125 mm, and an oil flow up to 210 L/min.

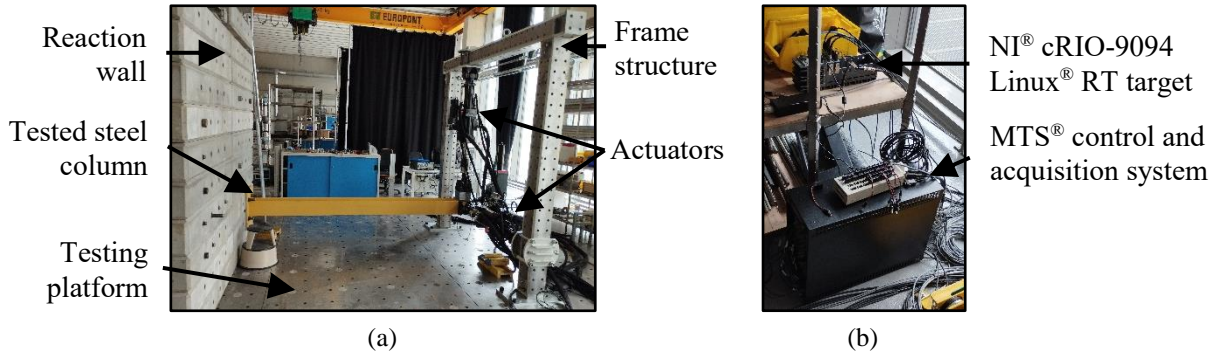


Figure 4: Experimental setup (a) and focus on the MTS® system and the Linux® RT target (b).

A mixed Proportional Integrative (PI) procedure set with $P = 15$ and $I = 5$ was used by a MTS® system that dealt with analog data to control the actuators in real-time, as described in Figure 5. The forces applied at the top of the steel column did not exceeded 12 kN on the present case study, which is 21 times lower compared to the maximum capacity of the actuators. Thus, no advance tuning procedures (e.g., cascade, or feed forward) were needed.

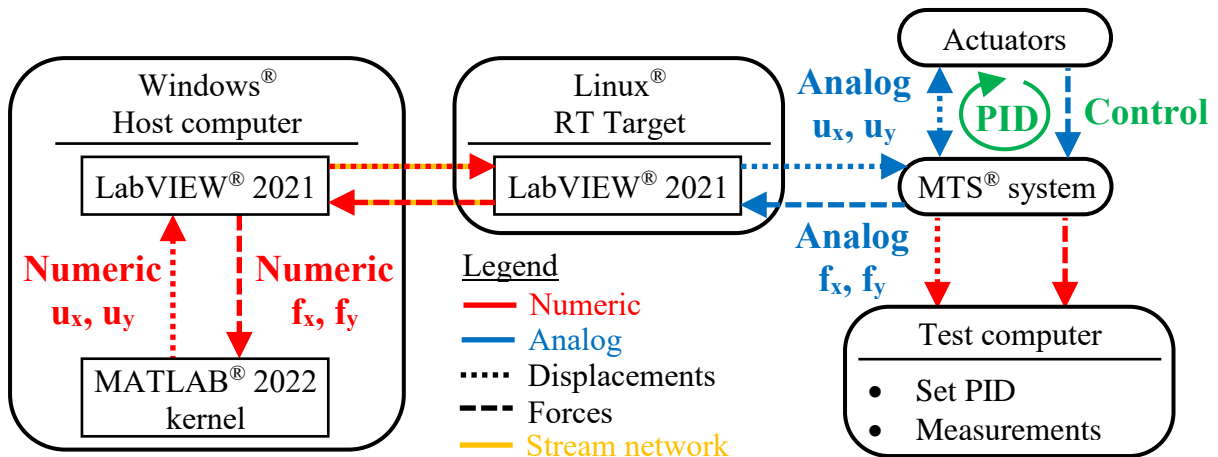


Figure 5: Data exchanges between the components of the experimental setup.

Simultaneously, an Intel® Core™ i7-12800H CPU @ 3.40 GHz and 32 GB RAM Windows® host computer dealing with numerical data ran the nonlinear dynamic analysis on the simulated substructure using a MATLAB® 2022 kernel, as described in Section 5.2. Both systems were connected by a National

Instrument® CompactRIO 9049 Linux® RT target (see Figure 4 (b)) writing, reading, and converting data quasi-instantaneously (i.e., in approximately 10 μ s per time step). The RT target converted the commands of the actuators from numeric to analog, and the restoring forces sent to the host computer from analog to numeric. The host computer and the RT target communicated in real time through a lossless stream network sending data to a LabVIEW® 2021 interface.

5. Applications

5.1. CPU time-savings using a HROM

The POD and UDEIM modal bases were built using a set of 1680 displacement and force snapshots selected every 10 ms according to the sampling period of the ground motion. All the snapshots (i.e., training data) were computed using the results of an offline dynamic analysis performed on the full structure under hybrid test conditions. An implicit Newmark method was used with a Newton-Raphson algorithm for this purpose, while the α -OS method was applied during the HiL RT hybrid test.

A sensitivity analysis was first performed to find the lowest value of the number n of POD modes guaranteeing a satisfactory accuracy of the result. When n was set, a second sensitivity analysis was then carried out to define the number of elements in the RID. All calculations were performed on the host computer described in Section 4.2 using custom procedures implemented in MATLAB® software. The reduced solutions are compared to the FOM in Figure 6 using the strain energy error ε_{Ed} defined in (7), where E_d^{FOM} is the strain energy of the implicit Newmark FOM, ΔE_d is the difference in strain energy, N_t is the number of time intervals, Δt is the time step, $\Delta \mathbf{u} = \mathbf{u} - \mathbf{u}^{FOM}$ is the difference in displacements, and $\Delta \mathbf{r} = \mathbf{r} - \mathbf{r}^{FOM}$ is the difference in restoring forces.

$$\varepsilon_{Ed} = \frac{\|\Delta E_d\|}{\|E_d^{FOM}\|} 100 \% \quad \text{with} \quad \|\Delta E_d\| = \frac{1}{2N_t\Delta t} \int_0^{N_t\Delta t} |\Delta \mathbf{u}^T(t)\Delta \mathbf{r}(t)| dt \quad (7)$$

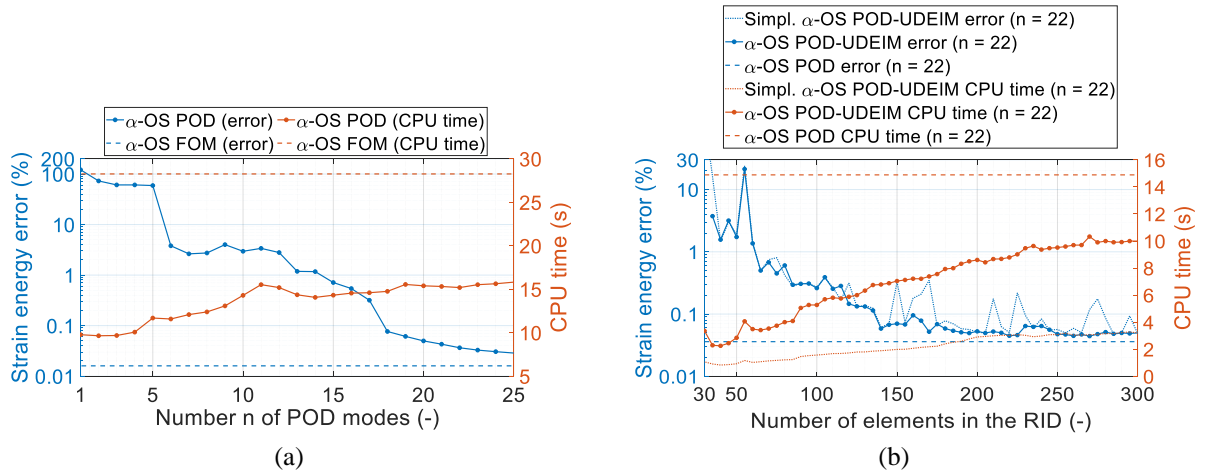


Figure 6: Error and online CPU time versus: the number of POD modes (POD) (a), and the number of elements in the RID with 22 POD modes (POD-UDEIM) (b).

Figure 6 (a) shows that the error does not exceed 0.04 % using the 22 POD modes defined by the highest singular values. Figure 6 (b) then proves that the online CPU time can be further reduced using a UDEIM procedure with a RID including 140 elements (~ 32 % of the mesh, see Figure 7 (a)). The resulting online phase lasts 6.67 s and proceeds accurately in less than 4 ms per time step (i.e., above the real time). Further simplifications (e.g., increasing the local strain increments of the concrete material law from 10^{-5} m/m to 10^{-4} m/m, or not updating the steel fibers properties since they remain elastic in the present case study) makes it possible to reach the same accuracy with an online phase lasting 2.01 s

(i.e., approximately 1.2 ms per time step, see the orange dotted curve in Figure 6 (b)). The horizontal displacement of the common node (see Figure 2 (a)) plotted in Figure 7 (c) along the x -axis shows that the simplified POD-UDEIM HROM agrees well with the FOM despite the appearance of material nonlinearities on 354 damaged elements (see the colored lines in Figure 7 (b)).

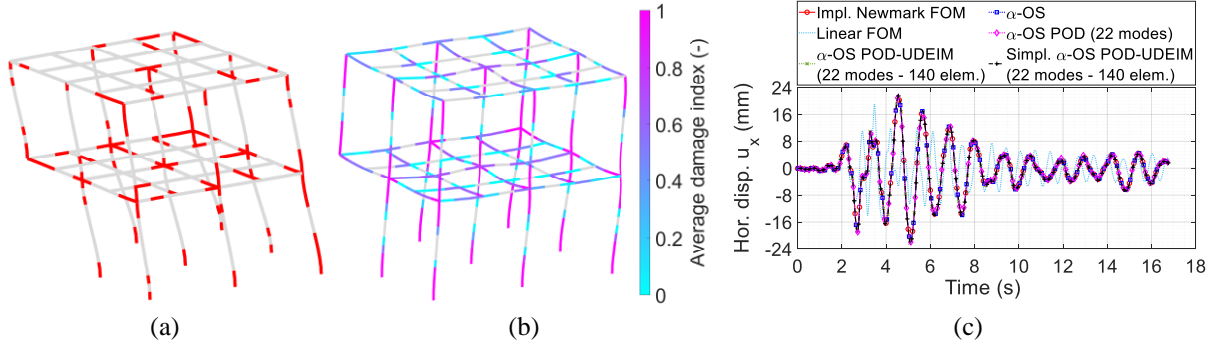


Figure 7: First POD mode and RID made of 140 beam elements (see the red lines) (a), final damage index on the FOM (354 damaged elements) (b), and horizontal displacement of the common node along the x -axis (c).

5.2. Method used to implement the finite element functions in the HiL procedure

The finite element functions need to be directly called from the acquisition software during HiL hybrid tests. Several approaches are available in LabVIEW®, but their efficiency is still an open question in the case of RT hybrid tests involving high dimensional nonlinear models. LabVIEW® proposes to either use an interpreted MATLAB® script (i.e., MathScript®), a kernel running MATLAB® functions, compiled C shared libraries, or .NET assemblies. In this section, all these methods are compared on the Benchmark case study in Section 4.1. The finite element functions were deployed on the Windows® host computer and the RT target when the device compatibility allowed it (e.g., Shared libraries, or MathScript®). The analysis was carried out from 0 to 30 s with a time step of 10 ms. The delay due to the solving process is plotted versus time in Figure 8, while the average delays are summarized in Table 1.

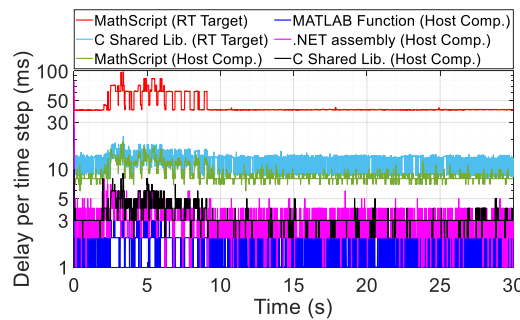


Figure 8: Delay per time step.



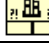
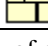
Method	Symbol	Average delay (ms)	
		Host computer	RT Target
MathScript®		8.9	44.6
Call MATLAB® functions		1.5	-
C shared library		3.3	12.4
.NET assembly		2.6	-

Table 1: Average delay of each method in LabVIEW®.

Calling MATLAB® functions in the Windows® host computer was by far the most efficient strategy with average and maximum delays of 1.5 ms and 3.0 ms, respectively. The vectors and the matrices remained in the MATLAB® kernel as persistent variables so that few data were exchanged with LabVIEW®. As 7 ms to 9 ms can be saved for the actuators, MATLAB® function calls were thus used to perform the RT hybrid test presented in Section 4.

5.3. Experimental results

The RT hybrid test was performed from 0 to 30 s, with commands updated on the Windows® host computer and sent to the actuators every 10 ms using the Linux® RT target. The data acquisition was ensured by the MTS® system at a sampling frequency of 2^{10} Hz (i.e., every 0.97 ms). The commands

and the horizontal displacements of the actuators are plotted in Figure 9 (a) and (b) along the x and y -axes, respectively. Both are compared to the theoretical and PsD responses with a factor 10 between the real and the deferred times.

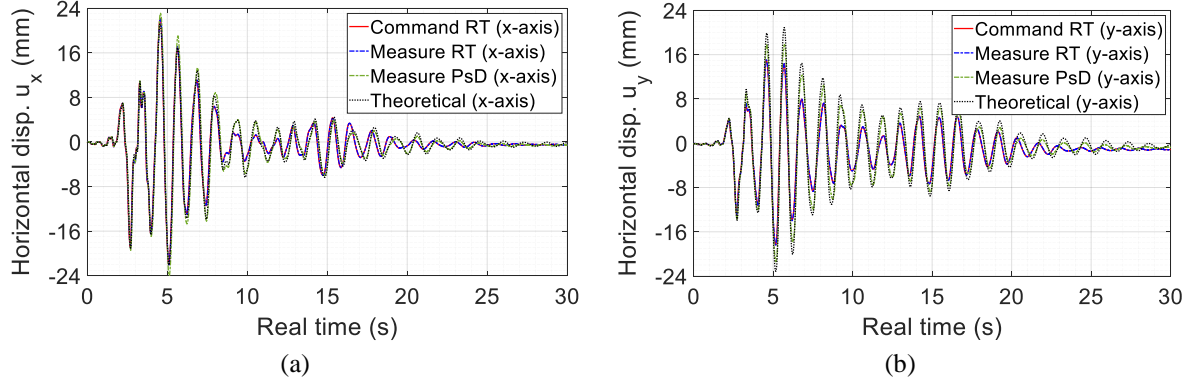


Figure 9: Commands, experimental, and theoretical values of the displacements applied by the actuators at the top of the steel column: x -axis (a), and y -axis (b).

The results show that measures (blue curves) almost perfectly agreed with commands (red curves) on both actuators, despite a residual delay of 9 ms that was not significant as the dynamics of the numerical model did not exceed 1.5 Hz (see Figure 10 (b)). The displacement along the x -axis was also in accordance with its theoretical and PsD values, even if slight variations appeared after the strong motion phase of the earthquake. This statement was not true along the y -axis, where the displacement exhibited a lower amplitude than expected. This could be due to nonlinearities in assemblies (e.g., gaps, contacts, or friction), undesirable steel frame dynamics (see Figure 4 (a)), inertial forces due to the mass of the vertical actuator, or interactions between components on the setup (e.g., steel frame, or specimen).

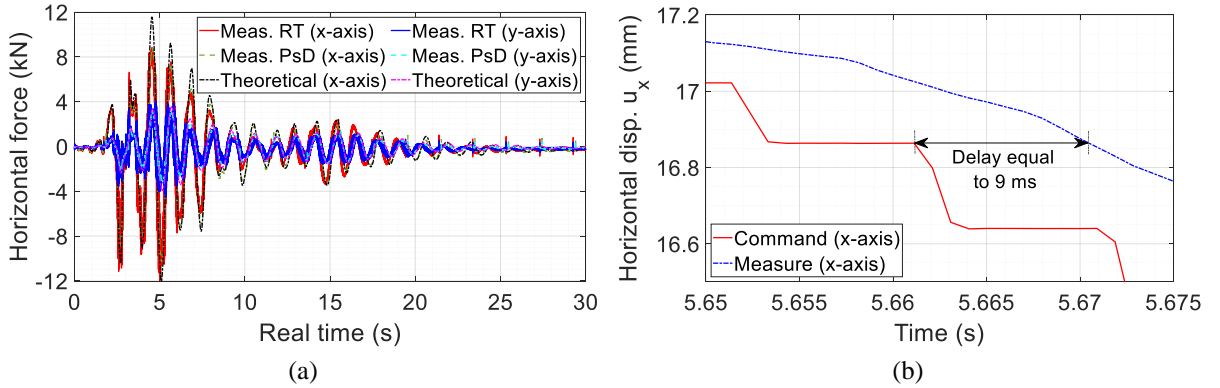


Figure 10: Experimental and theoretical values of the restoring forces (a), and delay in servo-hydraulic systems by comparison between the command and the measure along the x -axis (b).

Noise on force sensors may also have led to errors as its amplitude exceeded 1.5 kN during the strong motion phase (see Figure 10 (a) at time 5 s) due to a stiff coupling between actuators that generated shocks and jerks. All these phenomena added undesirable frequency contents to forces feedbacks, which activated high-order modes on the model that significantly changed its dynamics. Further improvements (e.g., feedforward predictor, filtering, delay compensation between systems, or interpolation on commands) consequently need to be investigated to minimize errors on displacement and force entries.

6. Conclusions

This paper presented a bidirectional real-time hybrid test on a steel column virtually connected to a two-story reinforced concrete structure under earthquake conditions. Nonlinearities were introduced in

Timoshenko multi-fiber beam elements using damage and elastic-plastic laws that modeled the concrete and the steel fibers, respectively. A POD-UDEIM hyper-reduced order modeling method first decreased the computational cost of the nonlinear model. The high dimensional system, initially made of 2382 free DOFs, was reduced on a basis of 22 POD modes, while the restoring force vector was approximated using a RID made of 140 elements (i.e., 32 % of the mesh). Further simplifications (e.g., increasing the local strain increments in the concrete material law, or not updating the properties of the steel fibers) made it possible to accurately run the dynamic analysis with a delay of approximately 1.2 ms per time step, which was far above the sampling period of the ground motion (i.e., 10 ms). A Benchmark comparison of the methods available in LabVIEW® to run FEM analyses then showed that calling a MATLAB® kernel running on the Windows® host computer is the best strategy, with delays that did not exceed 3.0 ms for the case under study. The procedure thus saved enough time to allow actuators reaching their command in real time, despite using a simulated substructure modeled by a costly nonlinear numerical model. As errors still remained on the experimental setup (e.g., frequency shift, and amplitude drops), improvements (e.g., feedforward predictors, or filtering) are currently investigated to reduce uncertainties (e.g., noises), while a test on a reinforced concrete column is currently under study.

References

- [1] Buchet P and Pegon P 1994 PsD Testing with Substructuring: Implementation and Use *Special publication ISPR A* 1 94.25
- [2] Nakashima M, Kato H and Takaoka E 1992 Development of real-time pseudo dynamic testing *Earth. Eng. and Struct. Dyn.* **21**(1) 79-92
- [3] Pegon P and Pinto V 2000 Pseudo-dynamic testing with substructuring at the ELSA Laboratory *Earth. Eng. and Struct. Dyn.* **29** 905-925
- [4] Nguyen T 2012 *Analyses du Comportement de Rupteurs Thermiques sous Sollicitations Sismiques (PhD Thesis)* (Cachan: ENS Cachan)
- [5] Souid A, Delaplace A, Ragueneau F, and Desmorat R 2009 Pseudo-dynamic testing and nonlinear substructuring of damaging structures under earthquake loading *Eng. Struct.* **31**(5) 1102-1110
- [6] Lebon G 2011 *Analyse de l'Endommagement des Structures de Génie Civil : Techniques de Sous-structuration Hybride Couplées à un Modèle d'Endommagement Anisotrope (PhD Thesis)* (Cachan: ENS Cachan)
- [7] Moutoussamy L 2013 *Essais Hybrides en Temps Réels sur Structures de Génie Civil (PhD Thesis)* (Cachan: ENS Cachan)
- [8] Ayoub N, Deü J-F, Larbi W, Pais J and Rouleau L 2022 Application of the POD method to nonlinear dynamic analysis of reinforced concrete frame structures subjected to earthquakes *Eng. Struct.* **270** 114854
- [9] Tiso P and Rixen D J 2013 Discrete empirical interpolation method for finite element structural dynamics *Nonlinear Modelling and Applications* vol 2 (New York: Springer) 53-65.
- [10] Hilber H, Hugues T and Taylor R 1977 Improved numerical dissipation for time integration algorithms in structural dynamics *Earth. Eng. and Struct. Dyn.* **5**(3) 282-292.
- [11] Bodnar B, Larbi W, Titirla M, Deü J-F, Gatuingt F and Ragueneau F 2022 Modelling of a PsD hybrid test on a RC column/beam junction combining a multifibre beam model and a POD-ROM approach *Comp. Mod. of Con. Struct. Euro-C 2022 (Vienne)*, ed Meschke, Pichler and Rots pp 414 - 423.
- [12] Combescure D, Pegon P and Magonette G 1995 Numerical investigation of the impact of experimental errors on various pseudo-dynamic integration algorithms *Proc. of the 10th Eu. Conf. on Earth. Eng.* Duma G (Rotterdam: Balkema) pp 2479-2484.
- [13] Davenne L, Ragueneau F, Mazars J and Ibrahimbegovic A 2003 Efficient approaches to finite element analysis in earthquake engineering *Comp. and Struct.* **81** 1223–1239.
- [14] Richard B and Ragueneau F 2013 Continuum damage mechanics based model for quasi brittle materials subjected to cyclic loadings: Formulations, numerical implementation and applications *Eng. Fract. Mech.* **98** 383-406.